International Journal of Information, Control and Computer Sciences
ISSN: 2517-9942
Vol:9, No:6, 2015

Face Recognition Using Discrete Orthogonal Hahn Moments

Fatima Akhmedova, Simon Liao

Abstract—One of the most critical decision points in the design of a face recognition system is the choice of an appropriate face representation. Effective feature descriptors are expected to convey sufficient, invariant and non-redundant facial information. In this work we propose a set of Hahn moments as a new approach for feature description. Hahn moments have been widely used in image analysis due to their invariance, non-redundancy and the ability to extract features either globally and locally. To assess the applicability of Hahn moments to Face Recognition we conduct two experiments on the Olivetti Research Laboratory (ORL) database and University of Notre-Dame (UND) X1 biometric collection. Fusion of the global features along with the features from local facial regions are used as an input for the conventional k-NN classifier. The method reaches an accuracy of 93% of correctly recognized subjects for the ORL database and 94% for the UND database.

Keywords—Face Recognition, Hahn moments, Recognition-by-parts, Time-lapse

I. Introduction

IF we try to imagine how different our life would be without the ability to memorize and recognize human faces, we will realize the exceptional importance of automatic face recognition for the progress of Artificial Intelligence. Since 1964 when the first attempt of semi-automatic facial recognition was made [1], a lot of effort has been put into achieving human-level performance. However, the recognition function, which is natural and trivial for the human brain, is much more difficult for machines. Computers perform well with static, controlled "mug-shot" identification, but when it comes to an uncontrolled one, the efficiency drops significantly due to the multiple variations presented in different images of the same person. Various poses, expressions, and lighting conditions greatly affect the biometric signature of a subject. To address this problem researchers withdrew the idea of using absolute geometric distances between facial parts as feature descriptors and began to look for more complex, yet more invariant attributes.

In 1990, Kirby and Sirovich [2] proposed the eigenfaces as a new, more robust technique. The algorithm is based on the use of basic statistical characteristics. An $N \times N$ image is represented as a sum of weighted eigenvectors, linearising the two-dimensional image into a vector of size N^2. Then, Principal Component Analysis (PCA) [3] is employed in order to reduce the dimensionality of the final feature set. PCA optimizes the existent high-dimensional space in the sense that the remaining data possess the most generalized information about the original images. As the dimensionality reduction is performed only for training set, this method is proved to be very fast, when testing new face images. However, in [4] Matthew Turk and Alex Pentland found that Eigenfaces are greatly affected by non-homogeneous conditions. The recognition rate drops from 84% of accuracy, possessing images of the same size to 64%, when size variations are presented.

Linear Discriminant Analysis (LDA) (also called Fisherfaces) [5] proposed in 2004, is generally superior to PCA because of the selection of the more robust feature subsets. It allows finding an optimal projection of the image onto the feature space so as to minimize the intraclass and maximize the interclass distance in the feature space. LDA shows a high recognition rate (about 94%) under different operational scenario conditions such as illumination and face expressions. Nevertheless, the linearity of methods like Eigenfaces/PCA, Fisherfaces/LDA assumes that they actually exploit only first and second order statistics. However, in [6] Bartlett Marian et al prove that first and second order statistics possess only aptitude-spectrum of an image, while experiments show that the human mechanism of recognition is primarily based on the phase-spectrum. Consequently, these methods might preserve redundant facial information, which impacts negatively the algorithm performance as well as computation time.

As one of the alternatives of the linear methods Elastic Bunch Graph Matching (EBGM) was proposed [7]. EBGM represents individual faces using graph architecture. An image graph representing an image contains nodes located at facial landmarks such as the pupils or the corners of the mouth. The face identification is performed by matching a new image structure with each graph in the training set, and the best match specifies the identity of person.

In the last decade three-dimensional recognition methods have become popular as they provide better robustness compared to two-dimensional techniques. A typical 3D face identification algorithm derives feature sets not directly from a 2D face image, but from a 3D model generated from it. Having a 3D facial model allows face images to be acquired from different rotation angles as well as head poses. It grants 3D methods a significant advantage over static 2D techniques. The main drawback of 3D methods is the computational cost of automatic 3D model creation as well as the often poor quality of the 3D images affecting the recognition rate.

Another holistic approach to the problem was to employ orthogonal moments [8] as feature descriptors. These moments

Fatima Akhmedova is with the Department of Applied Computer Science, the University of Winnipeg, Winnipeg, MB R3B 2E9, Canada e-mail: akhmedova-f@webmail.uwinnipeg.ca.

Simon Liao is with the University of Winnipeg, Winnipeg, Canada, since 1991. He is currently a professor in the Department of Applied Computer Science. Dr. Liao received the BSc degree in 1982 from Beijing Normal University, Beijing, China, and the MSc and PhD degrees in electrical and computer engineering from the University of Manitoba, Winnipeg, Canada, in 1988 and 1993, respectively. His research interests include pattern recognition, computer vision, and image processing.

are defined over the set of orthogonal polynomials and their orthogonality assures the non-redundancy of the feature set. In [9] the continuous orthogonal Zernike moments are utilized for feature description of face images taken over a time lapse, demonstrating moment approach to be a promising instrument for Face Recognition. However, since Zernike moment kernels are polynomials of continuous variables defined over a complex plane, numerical approximation and image coordinates transformation are required. It leads to an extra computational complexity as well as discretization error. To overcome the drawbacks of the continuous moments, Mukundan et al. proposed a set of discrete orthogonal moments based on the discrete Tchebichef polynomials [10]. Using these basis functions eliminates the need for numerical approximation, but at the same time preserves the orthogonality property. Tchebichef moments retain global image characteristics, whereas Krawtchuk moments [11] are capable of expressing an image locally. Both of them showed good results in various applications from Image Reconstruction to Face Recognition [12], [13].

This research focuses on the effectiveness of discrete orthogonal Hahn moments [14] as feature descriptors. The set of Hahn moments becomes Tchebishef or Krawtchuk moments depending on how the specific parameters of the Hahn kernel polynomials are set. Namely, Hahn moments are a general case of Tchebishef and Krawtchuk moments, and thus are able to retain global and local image characteristics. This is a particularly useful quality of Hahn moments, because it allows us to perform not only conventional appearance-based recognition, but also "recognition-by-parts", i.e. recognition by local facial regions. Moreover, the combination of global and local Hahn moments can provide a more powerful feature set.

To assess the performance of Hahn moment feature description we created a face recognition system which uses holistic (global moments), compositional (local moments) and hybrid (fusion of the global and local moments) approaches for feature extraction and k-nearest neighbour classifier for classification (Section III). We tested the system on the ORL face database [15] which contains 400 images presenting variability of expression, head pose and illumination, and obtained 93% of correctly recognized samples using hybrid approach (Section III.A). Furthermore, the proposed system efficiency was tested on the UND database [16], [17]. A particular difficulty in utilizing this database is that the images were taken over a time lapse. Thus, appearances of the subjects change significantly between sessions. Nevertheless, the recognition of 20 randomly selected individuals resulted in 94% rate in the hybrid mode (Section III.B). Finally, we provide the analysis of Hahn moments shortcomings and some insights on how to overcome them (Section IV).

II. Discrete Orthogonal Hahn Moments

Generally, moments can be considered as scalar values which describe a function in a way of capturing its substantial features. Mathematically, they are thought to be "projections" of a function onto a polynomial basis [18].

The definition of a general moment $M_{pq}^{(f)}$ of an image $f(x,y)$ where p,q are non-negative integers and $r=p+q$ is called the order of the moment is given as

$$M_{pq}^{(f)} = \iint_D \rho_{pq}(x,y) f(x,y)\, dx\, dy \tag{1}$$

where $\rho_{00}(x,y), \rho_{10}(x,y), ..., \rho_{ij}(x,y)$ are polynomial kernel functions defined on D. Hence, given a digitized image $f(x,y)$ of size $N \times M$, for discrete moments we have the following notation:

$$M_{nm}^{(f)} = \sum_{x=0}^{N-1} \sum_{y=0}^{M-1} \rho_n(x,N) \rho_m(y,M) f(x,y) \tag{2}$$

Different types of the basis polynomials $\rho_{nm}(x,y)$ produce different moment sets. To get Hahn moments we should employ Hahn polynomials $h_n^{(\mu,\nu)}(x,N)$, which are defined as follows

$$h_n^{(\mu,\nu)}(x,N) = (N+\nu-1)_n (N-1)_n \times \\ \times \sum_{k=0}^{n} (-1)^k \frac{(-n)_k (-x)_k (2N+\mu+\nu-n-1)_k}{(N+\nu-1)_k (N-1)_k} \frac{1}{k!} \tag{3}$$

where $(a)_k = a(a+1)(a+2)...(a+k-1) = (a+k+-1)!/(a-1)!$ is the Pochhammer symbol and parameters $\mu > -1, \nu > -1$ specify the shape of the polynomials. Orthogonality condition for Hahn polynomials is expressed by

$$\sum_{x=0}^{N-1} w(x) h_n^{(\mu,\nu)}(x,N) h_m^{(\mu,\nu)}(x,N) = d_n^2 \delta_{mn} \tag{4}$$

Here δ_{mn} is the Dirac impulse symbol, d_n^2 represents the square norm given by

$$d_n^2 = \frac{\Gamma(2N+\mu+\nu-n)}{(2N+\mu+\nu-2n-1)\Gamma(N+\mu+\nu-n)} \times \\ \times \frac{1}{\Gamma(N+\mu-n)\Gamma(N+\nu-n)\Gamma(n+1)\Gamma(N-n)} \tag{5}$$

and $w(x)$ denotes the weight function

$$w(x) = [\Gamma(x+1)\Gamma(x+\mu+1)\Gamma(N+\nu-x)\Gamma(N-x)]^{-1} \tag{6}$$

where $\Gamma(a) = (a-1)!$ is the gamma function.

Considering these equations, it is obvious that the values of the Hahn polynomials dramatically grow as the order increases. Consequently, they are technically inappropriate for moment computation. To overcome numerical instability, the Hahn polynomials are scaled by a factor, typically using the square norm and the weight function. Hence, we obtain weighted Hahn polynomials expressed as

$$\tilde{h}_n^{(\mu,\nu)}(x,N) = h_n^{(\mu,\nu)}(x,N) \sqrt{\frac{w(x)}{d_n^2}}, \tag{7}$$

where $n = 0, 1, ..., N-1$. In such case, the orthogonality condition transforms to an equation of the form

$$\sum_{x=0}^{N-1} \tilde{h}_n^{(\mu,\nu)}(x,N) \tilde{h}_m^{(\mu,\nu)}(x,N) = \delta_{mn} \tag{8}$$

where $n, m = 0, 1, ..., N-1$. Finally, to compute Hahn moments of the digital image $f(x, y)$ using the weighted Hahn polynomials, the following expression is applied

$$H_{nm} = \sum_{x=0}^{N-1} \sum_{y=0}^{M-1} \tilde{h}_n^{(\mu,\nu)}(x, N) \tilde{h}_m^{(\mu,\nu)}(x, M) f(x, y) \quad (9)$$

Computational Cost and Recurrence Relations: The use of Hahn moments as feature descriptors can be very computational expensive because of the complexity of the polynomial equations. Operations like factorials and gamma functions slow down the system, and virtually make it inexpedient. However, the orthogonal moments can be computed recurrently, reducing computation time significantly. The recurrence relation of the Hahn polynomials has the following view

$$A\tilde{h}_n^{(\mu,\nu)}(x, N) = B\sqrt{\frac{d_{n-1}^2}{d_n^2}}\tilde{h}_{n-1}^{(\mu,\nu)}(x, N) + \\ + C\sqrt{\frac{d_{n-2}^2}{d_n^2}}\tilde{h}_{n-2}^{(\mu,\nu)}(x, N), n = 2, 3, ..., N-1 \quad (10)$$

where

$$A = -\frac{n(2N + \mu + \nu - n)}{(2N + \mu + \nu - 2n + 1)(2N + \mu + \nu - 2n)}, \quad (11)$$

$$B = x - \frac{2(N-1) + \nu - \mu}{4} - \\ - \frac{(\mu^2 - \nu^2)(2N + \mu + \nu)}{4(2N + \mu + \nu - 2n + 2)(2N + \mu + \nu - 2n)}, \quad (12)$$

$$C = \frac{(N - n + 1)(N - n + \mu + 1)}{(2N + \mu + \nu - 2n + 2)} \times \\ \times \frac{(N - n + \nu + 1)(N - n + \mu + \nu + 1)}{(2N + \mu + \nu - 2n + 1)}. \quad (13)$$

It is easy to compute the zero-order Hahn polynomial, using (3) and (7):

$$\tilde{h}_0^{(\mu,\nu)}(x, N) = \sqrt{\frac{w(x)}{d_0^2}} \quad (14)$$

Accordingly, the first-order Hahn polynomial is found by

$$\tilde{h}_1^{(\mu,\nu)}(x, N) = \Big\{(N + \nu - 1)(N - 1) - \\ - (2N + \mu + \nu - 2)x\Big\}\sqrt{\frac{w(x)}{d_1^2}} \quad (15)$$

A. Matrix notation

Most of the modern computing environments are equipped with fast matrix calculation modules. Therefore, it is thrifty to carry out all computations in the matrix notation to speed up the performance.

To obtain the Hahn image moment set in the matrix notation we use the following representation [19]

$$\mathbf{H} = \mathbf{H}_x^T \mathbf{f} \mathbf{H}_y \quad (16)$$

where $\mathbf{f}$ designates the image matrix of $N \times M$ size and

$$\mathbf{H}_x = \left[\tilde{h}_0^{(\mu,\nu)}(x, N), \tilde{h}_1^{(\mu,\nu)}(x, N), ..., \tilde{h}_N - 1^{(\mu,\nu)}(x, N)\right]^T$$

$$\mathbf{H}_y = \left[\tilde{h}_0^{(\mu,\nu)}(y, M), \tilde{h}_1^{(\mu,\nu)}(y, M), ..., \tilde{h}_M - 1^{(\mu,\nu)}(y, M)\right]^T$$

Each element $\tilde{h}_k^{(\mu,\nu)}(x, N)$ of these vectors is a vector itself defined as

$$\tilde{h}_k^{(\mu,\nu)}(x, N) = \left[\tilde{h}_k^{(\mu,\nu)}(0, N), \tilde{h}_k^{(\mu,\nu)}(1, K), ..., \tilde{h}_k^{(\mu,\nu)}(N-1, N)\right]$$

B. Parameter Selection

As it was mentioned, a Hahn polynomial has a pair of the parameters $\{\mu, \nu\}$ defining its shape. Consequently, for a Hahn moment H_{nm} of the order $n + m$ we have a set of parameters $\{\mu_1, \nu_1, \mu_2, \nu_2\}$ which controls the region of emphasis in an image. Here $\mu_1 = p_1 t_1$, $\nu_1 = (1 - p_1)t_1$, $\mu_2 = p_2 t_2$, $\nu_2 = (1 - p_2)t_2$ [14]. The values t_1, t_2 are responsible for adjusting global-local trade-off. The closer to zero they are, the more global coverage of the moments is. To extract local information, we should have $t_1 >> 2N$, $t_2 >> 2M$. Empirically derived, that the optimal values are equal to respectively $20N$ and $20M$. The arguments $p_1 = x_r/N, p_2 = y_r/N$ actually control the region of interest (ROI). Here $\{x_r, y_r\}$ are the coordinates of the centre of the coverage area. To demonstrate the selective feature extraction, we perform image reconstruction using Hahn moments [19] using different parameter sets. The result is shown below in Fig.1.

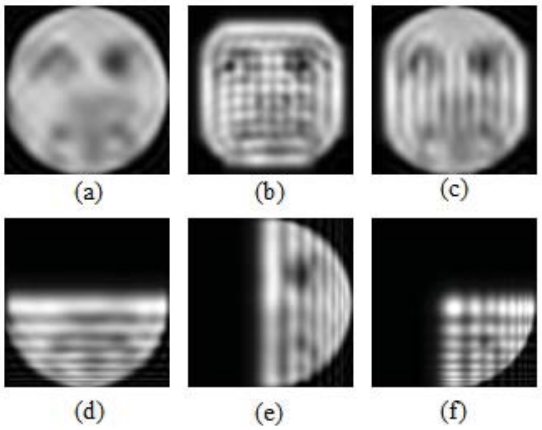

Fig. 1: The face image of size 90×85 is reconstructed using the Hahn moments of the orders $n = 19, m = 19$ and the parameters (a) global mode $\{\mu_1 = 0, \nu_1 = 0, \mu_2 = 0, \nu_2 = 0\}$, (b) local mode, image centre $\{\mu_1 = 180, \nu_1 = 170, \mu_2 = 180, \nu_2 = 170)\}$, (c) local mode, vertical orientation $\{\mu_1 = 0, \nu_1 = 0, \mu_2 = 180, \nu_2 = 170)\}$, (d) local mode, lower part $\{\mu_1 = 180, \nu_1 = 0, \mu_2 = 0, \nu_2 = 0)\}$, (e) local mode, right half $\{\mu_1 = 0, \nu_1 = 0, \mu_2 = 180, \nu_2 = 0)\}$,(f) local mode, right bottom $\{\mu_1 = 180, \nu_1 = 0, \mu_2 = 180, \nu_2 = 0)\}$

III. Proposed System and Experimental Results

The system presented in this work consists of three conventional stages: image preprocessing, feature extraction and classification, which is basically matching a new sample to the best candidate among the training set. Fig.2 illustrates the general structure of the system.

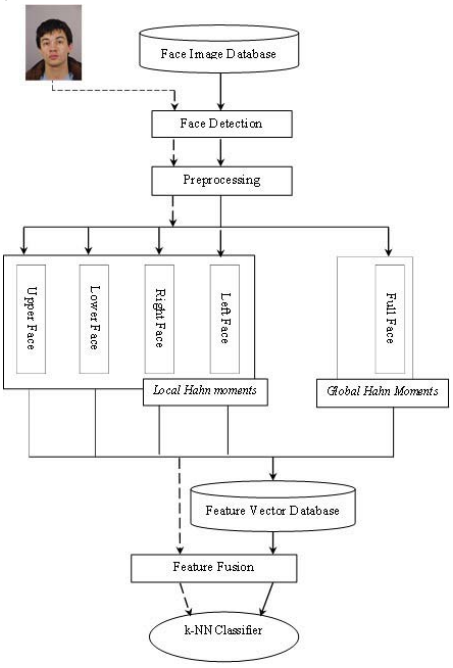

Fig. 2: The general scheme of the proposed system

Preprocessing stage includes face localization using the Viola-Jones object detection framework [20]. For simplification, we assume there is only one face per image. When the face region is located, its orientation normalization is performed. For this, firstly we find the eye ball regions using the same Viola-Jones algorithm, and then create a line connecting them. We define the image rotation angle as the line's slope angle relative to the x axis of the image. If the line is descending from left to right, the final rotation angle should be with the opposite sign. To get a natural oval facial region, we use a classical approximation algorithm [21] to fit an ellipse to the set of the coordinates that define the Viola-Jones rectangular face box. Finally, we resize all images to the universal size of 90×85.

As it is shown in Fig.2 there are five feature sets: one for the global moments and four for the local ones. To carry out "recognition-by-parts" we compute Hahn moments of the upper, lower, left and right halves of the face, using the following parameters:

TABLE I
Weighting Parameters of Hahn moments for Extracting Global and Local Features

ROI	μ_1	ν_1	μ_2	ν_2
Global	0	0	0	0
Left	0	0	0	170
Right	0	0	170	0
Top	0	180	0	0
Bottom	180	0	0	0

To find the best match for a testing entity among the feature vector database, we apply the well-known k-Nearest Neighbour (k-NN) classifier. k-NN classification is based on the property of "similarity". An object is classified to the group which the majority of its neighbours belong to. The measure of similarity or the property of neighbourhood is defined by a distance function. In our experiments we use Euclidean and Manhattan (city-block) distances. However, carrying out classification in the hybrid mode implies that we should combine local and global feature sets somehow. Fusion module sums up the Euclidean (or Manhattan) distances in the same manner as described in [13]. Having a pattern $z = [z^1, z^2, z^3, z^4, z^5]$, where z^1 is the global moment vector and z^2, z^3, z^4, z^5 are the local moment vectors, the summed normalized distance between the testing sample z and the training item $z_i = [z_i^1, z_i^2, z_i^3, z_i^4, z_i^5]$ is equal to

$$g(z, z_i) = \frac{\left\|z^1 - z_i^1\right\|}{\sum_{j=1}^{L}\left\|z^1 - z_j^1\right\|} + \frac{\left\|z^2 - z_i^2\right\|}{\sum_{j=1}^{L}\left\|z^2 - z_j^2\right\|} + \frac{\left\|z^3 - z_i^3\right\|}{\sum_{j=1}^{L}\left\|z^3 - z_j^3\right\|} + \frac{\left\|z^4 - z_i^4\right\|}{\sum_{j=1}^{L}\left\|z^4 - z_j^4\right\|} + \frac{\left\|z^5 - z_i^5\right\|}{\sum_{j=1}^{L}\left\|z^5 - z_j^5\right\|} \quad (17)$$

where L is the total number of the training samples. The formal definition of the k-NN classification rule is defined as follows

$$g(z, z_l) = g(z, z_j) \rightarrow h \in \omega_l \quad (18)$$

The training sample vector z is identified with the group of the minimum distance based on the similarity metric g. In other words, if k nearest neighbours of z in the training set belong to the class l, then z belongs to the class l either. The parameter k defining the sufficient number of the closest neighbours is usually adjusted empirically.

A. ORL experiment

ORL collection owned by AT&T Laboratories, Cambridge [22] consists of 400 images of 20 subjects. The pose, rotation and expression variations are broadly presented in the database. We randomly selected 200 images for the training and the remaining 200 samples for the testing, with no overlap between the sets. Fig. 3 shows original instances from the database as well as the output of the preprocessing.

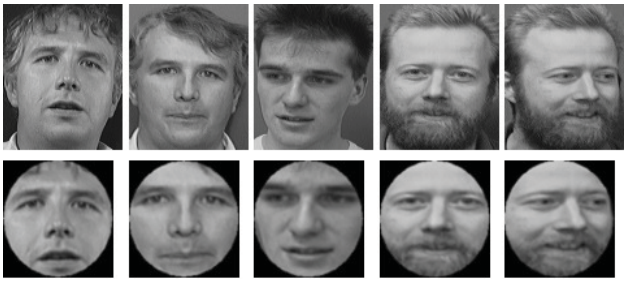

Fig. 3: Sample of images in the ORL database (top row) and the result of their preprocessing (bottom row)

Our prior goal was to empirically find the most optimal moment order, because lower orders can result in poor performance whereas higher order moments are computationally expensive and can also result in poor performance due to redundant information.

Fig. 4 demonstrates the obtained hit rates against the moment orders with the moment parameters set to 0 (global mode).

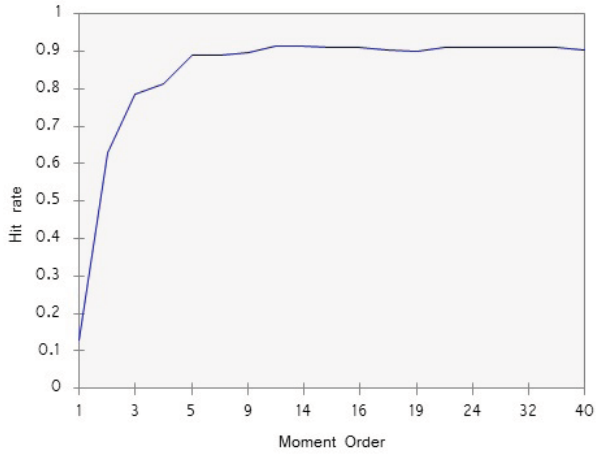

Fig. 4: The dependence of the correct recognition rate on the moment order

The system is capable of performing at the rate of 63% correctly recognized items with the moment orders $n = 2, m = 2$. Moreover, relatively low orders $n = 5, m = 5$ allows the algorithm to achieve 89% of the hit rate. It proves that Hahn moment feature descriptors possess very powerful discriminating properties. However, lower-order moments describe facial features rather generally, which results in getting smaller interclass distances between the data points. Further analysis of the graph leads us to conclude that the optimal value of the order is 12 with its 91.5% correctly recognized objects. The subsequent decrease in the quality of the classification is due to the fact that higher-order moments contribute more detailed information to the biometric signature of the entity. This in turn causes an increase of intraclass distances, and, as a consequence, an increase of misclassification. In the research [13] dedicated to the assessment of performance of the Krawtchouk moments, the authors choose orders 12, 19 and 29. In order to properly compare two discrete moment approaches, we opted for the same order values in the subsequent study.
To assess separately the holistic and compositional approaches, we computed the corresponding feature sets and performed the classifying without feature fusion. The results are given in Table II.

TABLE II
THE RESULTS OF GLOBAL AND LOCAL MODE RECOGNITION

Face region	Order n, m		
	12	19	29
Full face (global mode)	91.5%	90%	91%
Left	82%	86.5%	89%
Right	82%	86.5%	89%
Top	81%	86.5%	87.5%
Bottom	70.5%	78%	83.5%

From Table II we can clearly see that with the increase of the order, the gap between global and local mode effectiveness is reduced. The left and right facial half features are able to provide 86.5% of the hit rate with the order 19, and 89% with the order 29, which is only 2 % less than recognizing a full face. Thus, for the hybrid mode we may not combine all the feature vectors, but select the most efficient ones. We choose to perform various hybrid mode trials with the moments of order 19, because they are faster to compute and are still reasonably powerful. The results are compared with Krawtchuk moments and presented in the table below.

TABLE III
EFFECT ON THE RECOGNITION RATE OF VARIOUS FEATURE COMBINATIONS

Combination of features	Hahn moments	Krawtchuk moments
Full face (global mode)	90%	89.5%
Full + Top	88.5%	88.5%
Full + Bottom	88%	88%
Full + Left	89.5%	89.5%
Full + Right	92.5%	91.5%
Full + Top + Bottom	91.5%	91%
Full + Left + Right	92.5%	92.5%
Full + Top + Bottom + Left + Right	**93%**	**92.5%**

The highest hit rate of 93% is achieved with fully hybrid mode that combines the global and all the local feature vectors. However, the difference in performance between fully hybrid mode and the one using left and right facial halves is almost negligible. Another interesting observation is that recognition by full face and the right half is more efficient than with the left one, although individually they contribute equally.
Obviously, in general, Hahn moments tend to outperform Krawtchuk moments, but concerning "recognition-by-parts" the discrepancy is insignificant.

B. UND experiment

To reinforce efficiency of a biometric algorithm, we should verify it using more than only one database, otherwise the effectiveness of the algorithm might simply stem from its over-fitting to the input data. The University of Notre-Dame X1 biometrics collection was chosen for an additional testing. This database contains 2292 frontal face images from 82 subjects captured from 2002 to 2004. For the experiment we randomly selected 20 subjects. Each of them attended 10 acquisition sessions for each season. Hence, the first ten session images are used for training and the next ten images are used for testing. There is also no overlap between testing and training sets. Head rotation allowance is at most 15 degrees. The preprocessing stage is carried out in technically the same manner as in the previous experiment. In addition the images were converted to grayscale colour depth, but no histogram equalization was performed, as we wanted to assess the actual algorithm's robustness to the illumination variability. Sample input and preprocessed images of a single subject are given in Fig. 5.

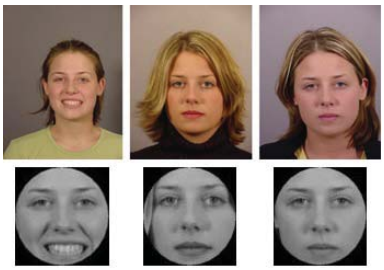

Fig. 5: Sample of images in the UND database (top row) and the result of their preprocessing (bottom row)

In the first experiment we computed feature vectors of up to order $n+m=19$ and carrying out classification with various feature set combinations. Furthermore, Manhattan distance was employed to determine the similarity between the data points. Manhattan distance, also called taxicab metric is a simple metric which measures distance following only axis-aligned directions. It is defined by

$$g((x_1,x_2),(y_1,y_2)) = |x_1-x_2|+|y_1-y_2| \tag{19}$$

for all points $P_1(x_1,y_1)$ and $P_2(x_2,y_2)$. Consequently, Euclidean norm in (17) is replaced by Manhattan norm, leading to the new expression for feature set fusion:

$$g(z,z_i) = \frac{|z^1-z_i^1|}{\sum_{j=1}^{L}|z^1-z_j^1|}+\frac{|z^2-z_i^2|}{\sum_{j=1}^{L}|z^2-z_j^2|}+\frac{|z^3-z_i^3|}{\sum_{j=1}^{L}|z^3-z_j^3|}+ \\ +\frac{|z^4-z_i^4|}{\sum_{j=1}^{L}|z^4-z_j^4|}+\frac{|z^5-z_i^5|}{\sum_{j=1}^{L}|z^5-z_j^5|} \tag{20}$$

The comparative results of the used metrics' performance is presented on the table below.

TABLE IV
EFFECT OF USING DIFFERENT SIMILARITY METRICS ON THE RECOGNITION RATE

Feature Set Combination	Distance	
	Euclidean	Manhattan
Global	85%	92.5%
Left	80%	85%
Right	80.5%	87%
Top	73%	72.5%
Bottom	69.5%	64%
Fully Hybrid	**89.5%**	90.5%
Global + Left + Right + Top	85%	91%
Global + Left + Right	87.5%	92.5%
Global + Top	85%	87%
Global + Bottom	86.5%	86%
Global + Left	83%	90.5%
Global + Right	88.5%	**94%**

The interesting outcome of the experiment is that using the less complex metric produces better results. Moreover, Manhattan distance classification using the whole face and its right half proved to be more robust than the complete hybrid set. Even utilizing only global moments gives the impressive hit rate of 92.5%. In addition, Manhattan distance computation is twice as fast compared to the computation of Euclidean distance, which is very important for the feasible design of biometric identification systems.

IV. CONCLUSION

This research proved the powerful descriptive capacity of Discrete Orthogonal Hahn moments. The accuracy of Hahn moment feature descriptors was assessed on the ORL and UND databases by using the hybrid identification scheme as well as individually holistic and compositional approaches. The obtained results show that generally Hahn moments outperformed Krawtchuk moments. Euclidean and Manhattan objective functions were employed in k-NN classfier and demonstrated significant discrepancy in recognition accuracy for the UND database images. Computation of higher-order Hahn moments ($n+m=19$) for a single grayscale testing image of size 90×85 takes 0.44 sec, which is sufficiently fast for the most applications.

As any other technique, utilizing discrete moments as feature vectors has its pitfalls. First of all, it is the predominance of empirically adjusted parameters of feature extraction. There is no formal relation which would define the most optimal moment order or the polynomial parameters. Another shortcoming is that in order to avoid complex preprocessing, we have to compute moment invariants [23] to achieve rotation and scale invariance. Therefore, the prospects of the future work are to find a formal definition of the optimal moment parameters in terms of their relation to the input data. Furthermore, the performance of Hahn moment feature description should be assessed with the other classification techniques, such as Support Vector Machine or fuzzy k-NN classifier. Finally, using Hahn moments as neural network input would provide a combination of nonlinear feature selection along with nonlinear classification.

REFERENCES

[1] Bledsoe, W. W. *The Model Method in Facial Recognition*, Technical Report PRI 15, Panoramic Research, Inc., Palo Alto, California, 1964
[2] M. Kirby and L. Sirovich. *Application of the Karhunen-Loeve procedure for the characterization of human faces*. IEEE Transactions on Pattern analysis and Machine Intelligence 12, 1990
[3] Jolliffe, I. T. *Principal Component Analysis*. Springer-Verlag. p. 487, 1986
[4] A. Pentland, T. Starner, N. Etcoff, N. Masoiu, O. Oliyide, and M. Turk. *Experiments with Eigenfaces*. Proc. Looking at People Workshop Int'l Joint Conf. Artifical Intelligence, 1993
[5] McLachlan, G. J. *Discriminant Analysis and Statistical Pattern Recognition*. Wiley Interscience, 2004
[6] Marian Stewart Bartlett, Javier R. Movellan, and Terrence J. Sejnowski *Face Recognition by Independent Component Analysis*. IEEE Trans Neural Netw. vol. 13(6), pages 14501464, 2002
[7] Laurenz Wiskott, Jean-Marc Fellous,Norbert Kruger, and Christoph von der Malsburg. *Face Recognition by Elastic Bunch Graph Matching*. Intelligent Biometric Techniques in Fingerprint and Face Recognition, Chapter 11, pages 355-396, 1999
[8] Arnold F. Nikiforov, Vasilii B. Uvarov, Sergei K. Suslov. *Classical Orthogonal Polynomials of a Discrete Variable*. Springer Series in Computational Physics, 1991
[9] Sajad Farokhi, Siti Mariyam Shamsuddin, Jan Flusser, Usman Ullah Sheikh. *Assessment of Time-Lapse in Visible and Thermal Face Recognition*. World Academy of Science, Engineering and Technology Vol.6, 2012
[10] Mukundan, R., Ong S.H., Lee P.A. *Image analysis by Tchebichef moments*. Image Processing, IEEE Transactions on, Vol.10 , Issue: 9, 2001
[11] Yap P.T., Paramesran R., Ong S.H. *Image analysis by Krawtchouk moments*. IEEE Trans Image Process. Vol. 12, pages 1367-77, 2003
[12] Sri dhar Dasari, Sridhar Dasari. *Face Recognition using Tchebichef Moments*.International Journal of Infromation and Network Security, Vol 1, No 4, 2012
[13] J Sheeba Rani, D Devaraj. *Face recognition using Krawtchouk moment*. Sadhana, Vol. 37, Issue 4, pages 441-460, 2012

[14] Pew-Thian Yap, Paramesran, R., Seng-Huat Ong. *Image Analysis Using Hahn Moments*. Pattern Analysis and Machine Intelligence, IEEE Transactions on, Vol. 29, Issue 11, 2007
[15] Ferdinando Samaria, Andy Harter. *Parameterisation of a Stochastic Model for Human Face Identification*. Proceedings of 2nd IEEE Workshop on Applications of Computer Vision, Sarasota FL, 1994
[16] P. J. Flynn, K. W. Bowyer, and P. J. Phillips. *Assessment of time dependency in face recognition: An initial study*. Audio and Video-Based Biometric Person Authentication, pages 44-51, 2003.
[17] X. Chen, P. J. Flynn, and K. W. Bowyer. *Visible -light and Infrared Face Recognition*. ACM Workshop on Multimodal User Authentication, pages 48-55, 2003
[18] Jan Flusser, Barbara Zitova, Tomas Suk. *Moments and Moment Invariants in Pattern Recognition*. ISBN: 978-0-470-69987-4, page 6, 2009
[19] Jian Zhou, Huazhong Shu, Hongqing Zhu, Christine Toumoulin, and Limin Luo. *Image Analysis by Discrete Orthogonal Hahn Moments*. Lecture Notes in Computer Science, Vol. 3656, pages 524-531, 2005
[20] Paul Viola, Michael Jones. *Robust Real-time Object Detection*. International Journal of Computer Vision, 2001
[21] Andrew Fitzgibbon, Maurizio Pilu, and Robert B. Fisher. *Direct Least Square Fitting of Ellipses*. Proc. of the 13th Internation Conference on Pattern Recognition, pages 253257, Vienna, 1996
[22] *http://www.cl.cam.ac.uk/research/dtg/attarchive /facedatabase.html*.
[23] Sayyouri M, Hmimid A, Qjidaa H. *Improving the performance of image classification by Hahn moment invariants*. Journal of the Optical Society of America, Vol. 30, Issue 11, pages 2381-2394, 2013